International Symposium
On Turbulence and Shear Flow
Phenomena (TSFP-8)
August 28 - 30, 2013 Poitiers, France

EFFECT OF ACTIVE CONTROL ON OPTIMAL STRUCTURES IN WALL TURBULENCE

B.Q. Deng, C.X. Xu, W.X. Huang and G.X. Cui
Department of Engineering Mechanics
Tsinghua University
Beijing 100084, P. R. China
xucx@tsinghua.edu.cn

Abstract

The effect of active control imposed at the wall on optimal structures in wall turbulence is investigated by using a linear transient growth model. When the detection plane of the control is located in the buffer layer, the transient growth of the near-wall structures can be suppressed, but the large scale motion can hardly be influenced as the Reynolds number increases, even when the control amplitude is enhanced. When the input signal for the control is detected in the logarithm region, the transient growth of the large-scale motions can be greatly suppressed, although a new peak occurs in the transient growth rate due to the strong blowing and suction at the wall. The results indicate that the flow information in the logarithmic region is crucial for constructing a control scheme to effectively manipulate the large-scale motions.

Introduction

Coherent structures are closely related to the generation of high skin friction in wall-bounded turbulent flows (Robinson, 1991; Kravchenko *et al.*, 1993). Therefore, a great many studies (Choi *et al.*, 1994; Collis *et al.*, 2004) have focused on the dynamics of the coherent structures for the purpose of turbulence control over the past decades. Besides the typical coherent structures in buffer layer, such as the low-speed streaks and the quasi-streamwise vortices which also exists in low-Reynolds number wall turbulence, large scale motions with characteristic spanwise and streamwise scales of $\lambda_z \approx O(h)$ and $\lambda_x \approx O(10h)$ (Tomkins & Adrian, 2003; Gnanpathisubramani *et al.*, 2005; del Alamo & Jimenez, 2003) occupy the logarithmic region in high Reynolds number wall-bounded turbulent flows (Adrian *et al.*, 2000; Abe *et al.*, 2004; Hoyas & Jimenez, 2006). As the Reynolds number increases, the large scale structures carry a more significant fraction of the Reynolds stress (Hoyas & Jimenez, 2006), and play a more important role in turbulence production and skin friction generation. Therefore the effective manipulation of the large scale structures is crucial for a successful control of high-Reynolds number wall-bounded turbulent flows.

The linear theory for flow instability is an useful tool for the study of coherent structures (del Alamo & Jimenez, 2006). Investigation of the linearized N-S equations yields that the stable disturbance on laminar flow can undergo transient growth before its exponential decaying. This can be attributed to the non-orthogonality of the eigenfunctions of the Orr-Sommerfeld and the Squire equations. Due to the non-orthogonality, different stable modes can interact with each other to achieve a transient growth in a short time period. In the case of the laminar channel flow, the optimal initial perturbations are uniform streamwise vortices, and the optimally amplified structures are streaks (Butler & Farrell, 1992). The streaks resulting from the transient growth of perturbations is produced by the lift-up effect of the streamwise vortices. Since the mean turbulent velocity profile in channel flow is linearly stable, the transient growth mechanism is crucial for the generation of the flow structures. Butler & Farrell (1993) found that the optimal structures were also streamwise vortices and streaks in turbulent cases, and the spanwise spacing between the streaks were $\lambda_z = 3h$. They also attained the optimal structures with spacing of $\lambda_z^+ \approx 100$ by constraining the transient growth time to the eddy turnover time in the near-wall region. Recently, del Alamo & Jimenez (2006) and Pujals *et al.* (2009) considered the nonlinear influence of turbulent fluctuations by replacing the molecular viscosity by the total viscosity in the formulation of the governing equations for the linear perturbations, and obtained the optimal structures with both spanwise spacing of $\lambda_z^+ \approx 100$ and $\lambda_z = 4h$ without constraining the transient growth time. The previous works show that the linear transient growth model can capture the main characteristics of the flow structures in the fully developed turbulence. In a turbulent flow environment, the optimal structures are the most probable structures to grow and survive. Furthermore, Lim & Kim (2004) studied the transient growth of turbulent channel flow in the presence of the opposition control based on the same model as that used by Butler & Farrell (1993). They obtained a similar conclusion as that by direct numerical simulation: if the detection plane was located near enough to the wall, the transient growth rate under the control was smaller than that without control, whereas, if the detection plane was located farther away from the wall, the transient growth rate became larger than that without control. In Lim & Kim (2004)'s work, the Reynolds numbers were limited to be less than $Re_\tau = 400$ and only the near-wall structures were considered by limiting the transient growth time.

Therefore, the main purpose of the present work is to investigate the influence of the active control on flow structures at high Reynolds numbers, especially the large scale structures in the logarithmic region, by using the linear transient growth model proposed by Pujals *et al.* (2009).

Computation Model

In the present work, the mean velocity profile of turbulent channel flow is employed as the base flow, i.e., $\mathbf{U} = (U(y),0,0)$. By writing the perturbation velocity $\mathbf{u}$ into the form of $\mathbf{u} = \hat{\mathbf{u}}(\alpha,\beta,y,t)\exp\{i(\alpha x+\beta z)\}$, where α and β are the streamwise and spanwise wave numbers, respectively, the linearized equations for the perturbations proposed by Pujals *et al.* (2009) are

$$\begin{bmatrix} D^2-k^2 & 0 \\ 0 & 1 \end{bmatrix} \frac{\partial}{\partial t} \begin{bmatrix} \hat{v} \\ \hat{\omega}_y \end{bmatrix} = \begin{bmatrix} L_{os} & 0 \\ -i\beta\frac{DU^+}{D\eta} & L_{sq} \end{bmatrix} \begin{bmatrix} \hat{v} \\ \hat{\omega}_y \end{bmatrix}, \quad (1)$$

with

$$\begin{aligned} L_{os} &= -i\alpha[U^+(D^2-k^2) - \tfrac{D^2U^+}{D\eta^2}] \\ &+ \tfrac{1}{\mathrm{Re}_\tau}\{{\nu_T}^+(D^2-k^2)^2 + 2\tfrac{\partial {\nu_T}^+}{\partial\eta}(D^3-k^2D) + \\ &\tfrac{\partial^2 {\nu_T}^+}{\partial\eta^2}(D^2+k^2)\}, \end{aligned} \quad (2)$$

$$L_{sq} = -i\alpha U^+ + \frac{1}{\mathrm{Re}_\tau}(i\alpha {\nu_T}^+(D^2-k^2) + \frac{\partial {\nu_T}^+}{\partial\eta}D), \quad (3)$$

where D stands for $\partial/\partial\eta$, and $k^2 = \alpha^2+\beta^2$. The dimensionless parameters are defined as $\eta = y/h$, $U^+ = U/u_\tau$, where h is the half height of the channel and u_τ is the friction velocity. $\nu_T(y)$ is given by the Cess expression

$$\begin{aligned} \nu_T^+(\eta) = \frac{1}{2}\{1 + \frac{\kappa^2 Re_\tau^2}{9}(1-\eta^2)^2(1+2\eta^2)^2 \\ \times\{1-\exp[(|\eta|-1)Re_\tau/B]\}^2\}^{1/2} + \frac{1}{2}. \end{aligned} \quad (4)$$

The constants κ and B in equation (4) are chosen to be 0.426 and 25.4, respectively, which have been confirmed by Pujals *et al.* (2009). The base flow can be computed according to $dU^+(\eta)/d\eta = -Re_\tau\eta/\nu_T^+(\eta)$. The boundary conditions are specified at the wall as

$$\hat{v}_{wall} = 0, \quad \frac{\partial\hat{v}}{\partial\eta}|_{wall} = 0 \quad (5)$$

for the no control case. In the case of the opposition control, the blowing and suction on the wall are considered by the boundary condition as

$$\hat{v}_{wall} = -\hat{v}(y_d), \quad \frac{\partial\hat{v}}{\partial\eta}|_{wall} = 0. \quad (6)$$

The transient growth rate $G(t,\alpha,\beta)$ is defined as :

$$G(t,\alpha,\beta) = \sup_{E(0,\alpha,\beta)\neq 0}\frac{E(t,\alpha,\beta)}{E(0,\alpha,\beta)} \quad (7)$$

where $E(t,\alpha,\beta)$ is the kinetic energy of the perturbations at time t and $E(0,\alpha,\beta)$ is the energy at $t=0$. The maximum transient growth rate is the maximum value of $G(t,\alpha,\beta)$ in the entire time range,

$$G_{max}(\alpha,\beta) = \max_{t\geq 0} G(t,\alpha,\beta). \quad (8)$$

The initial perturbation which leads to G_{max} is referred to as the optimal structures.

The equations are discretized by a Chebyshev collocation method, and the maximum transient energy growth is computed by the method introduced in Schmid & Henningson (2001). According to the previous studies by Pujals *et al.* (2009), the numbers of collocation points used in the present study are in the range of $129 \sim 800$ for the Reynolds number $Re_\tau = 500 \sim 20000$. It is verified that the energy transient growth for the no control cases obtained in the present study is consistent with the results of Pujals *et al.* (2009).

Results and analysis

First the no control case at $Re_\tau = 1000$ is considered. Figure 1(a) and figure 2 show the maximum energy transient growth rates G_{max} and the optimal structures. The results are consistent with Pujals *et al.* (2009)'s : the maximum transient growth rate exists in the range of $\alpha < \beta$, and shows two peaks. The value of the outer peak, corresponding to a streamwise uniform structure with spanwise wavelength of $\lambda_z \approx 4h$, is about 10.5. The inner peak, corresponding to $\lambda_z^+ \approx 100$, takes the value of 3. The spanwise length scales corresponding to the outer and inner peaks are respectively consistent with the large scale motions in the logarithmic region and the near-wall coherent structures in turbulent channel flow. The transient growth process of the outer peak is as the following: the counter-rotating streamwise vortices with their centers located at the center of the channel capture energy from the mean flow and forms the streaks that penetrate into the near-wall region, as shown in figure 2(a). The process of the inner peak is similar as that of the outer peak except that the centers of the initial streamwise vortices are located at around $y^+ = 15$ and the maximum value of the amplified streaks are reached at $y^+ = 10$, as shown in 2(b).

Figure 1(b) shows the contours of G_{max} for the case of $y_d^+ = 15$ control at $Re_\tau = 1000$. In this control case, the inner peak is obviously diminished, and only the outer peak remains with unchanged location in the (α,β) plane. The optimal structures at the outer peak under the control is very close to the uncontrolled. Since the inner peak is relevant with the near-wall rolls and streaks, this result also indicates that the opposition control with $y_d^+ = 15$, which is considered to be the optimal detection location in terms of the maximum drag reduction rate, is very effective in suppressing the growth of the near-wall structures. This is consistent with the results

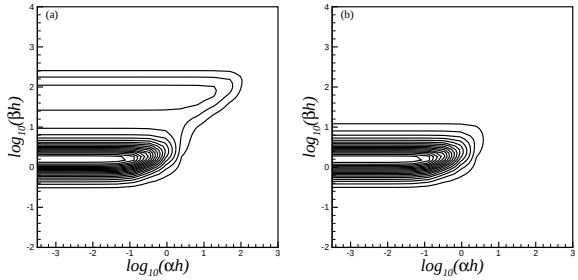

Figure 1. Contours of G_{max} for the (a) no control and (b) $y_d^+ = 15$ control cases at $Re_\tau = 1000$. Contour levels start from 1.0 with an increment of 0.5.

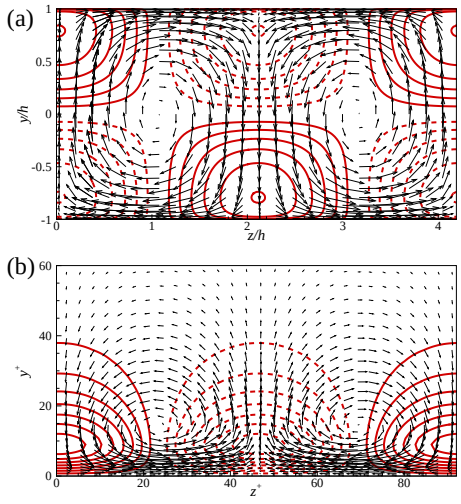

Figure 2. Vectors for optimal initial velocity field and contours for amplified streamwise velocity at the (a) outer peak and (b) inner peak in the no control case. The dashed line indicates negative streamwise velocity and the solid line represents positive streamwise velocity.

obtained in the direct numerical simulation of turbulent channel flow by Choi *et al.* (1994), although the present Reynolds number is much higher that that used by Choi *et al.* (1994). Notably, the control cannot clear off all the near-wall structures in real turbulent flow, while in the present linear model the inner peak of the transient growth vanishes completely under the control because of the neglecting of the nonlinear interaction between different scales. At $Re_\tau = 1000$, the control with $y_d^+ = 15$ only has trivial influence on the outer peak or the large scale structures.

The Reynolds number effect on the $y_d^+ = 15$ control is further considered. Because the peak value of the maximum transient growth is only reached at $\alpha = 0$ for both the no control and the $y_d^+ = 15$ control cases, therefore only the G_{max} for the streamwise uniform structures is shown in figure 3. For the no control cases as indicated by the solid lines in the figure, the outer peak and inner peak characteristics are the same as those in the work of Pujals *et al.* (2009)'s : the outer peak is located around $\beta h = 1.5$ and the peak value increases with the Reynolds number, while the inner peak exists at $\lambda_z^+ \approx 90$

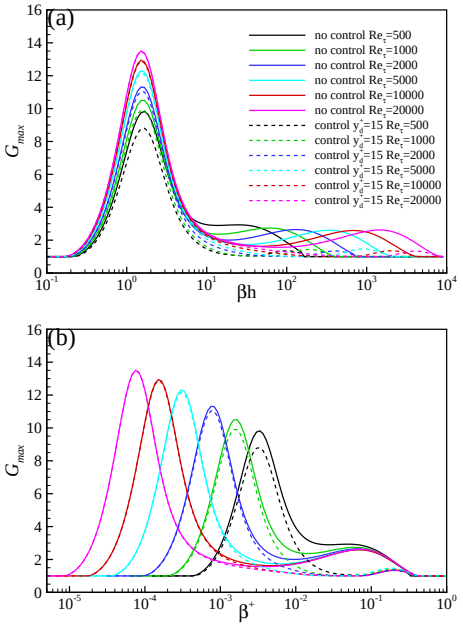

Figure 3. Distribution of G_{max} as a function of β for $\alpha = 0$ at $Re_\tau = 1000 \sim 20000$ in the cases of no control and $y_d^+ = 15$ control. (a) in wall unit ν/u_τ and (b) in outer length scale h.

and the peak value is independent of the Reynolds number, as shown in figure 3(a) and (b), respectively. The results for the $y_d^+ = 15$ control are shown by the dashed lines in 3. The outer peaks for the Reynolds numbers between 500 and 20000 are all located at $\beta h = 1.5$. However, the suppression of the peak values due to the control decreases as the Reynolds number increases. The outer peak value is almost unchanged provided $Re_\tau > 2000$. Because the detection location is measured in wall units and $y_d^+ = 15$ is located in the buffer layer, the vertical height corresponding to $y_d^+ = 15$ sharply decreases from $0.03h$ to $0.00075h$ as the Reynolds number increases from 500 to 20000. Moreover, the structures corresponding to the outer peaks are mainly located in the logarithm region, which is completely separated from the buffer layer at large enough Reynolds numbers. Therefore, the control limited in the near-wall region has less effect on the outer peak as the Reynolds number increases. Additionally, the optimal structures at the outer peak (not shown here) under the control only deviate from those of the no control cases very little. This agrees with the results of O.Flores & del Alamo (2007) that the roughness of the wall does not affect the existence and distribution of vortex clusters in the outer region, which can be considered as the large scale motions. The inner peaks for all the Reynolds numbers are suppressed by the control. As shown in the work of Pujals *et al.* (2009) and figure 2(b), the vertical velocity of the structures corresponding to the inner peak reaches the maximum value around $y_d^+ = 15$, so the control with $y_d^+ = 15$ can take significant effect.

The time at which the maximum transient growth is reached, T_{max}, is shown in figure 4 for different spanwise wavelength scaled in wall units. The $y_d^+ = 15$ control obviously diminishes the time of the transient growth around $\lambda_z^+ = 100$, which is consistent with the location of the inner

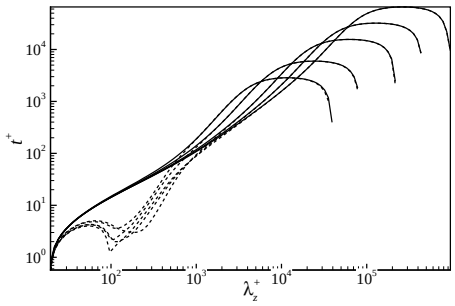

Figure 4. Variations of T_{max} as a function of λ_z^+ at $\alpha = 0$ for $Re_\tau = 500 \sim 20000$. Solid lines represent the no control cases and dashed lines stand for the $y_d^+ = 15$ control cases.

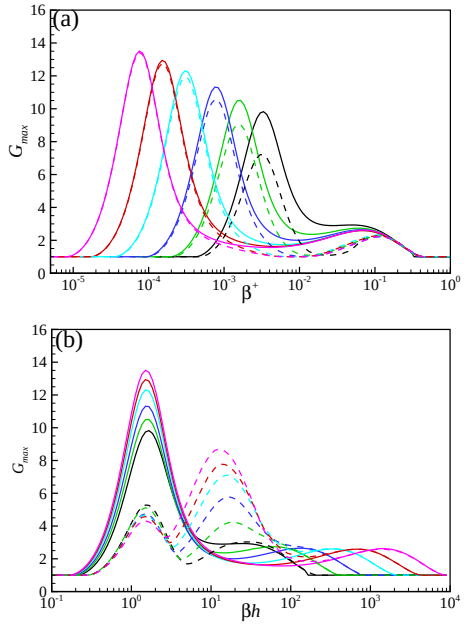

Figure 5. Distribution of G_{max} as a function of β for $\alpha = 0$ at $Re_\tau = 1000 \sim 20000$. (a) $y_d^+ = 30$ control, in wall unit ν/u_τ; (b) $y_d = 0.1h$ control, in outer length scale h.

peak in G_{max}. Beyond $\lambda_z^+ = 100$, the difference in the time between the no control and the $y_d^+ = 15$ control decreases as the spanwise wavelength increases. The control almost has no influence on the transient growth time at large scales when $\lambda_z^+ > 1000$. This confirms the results that the $y_d^+ = 15$ control can suppress the inner peak and the near-wall structures, but has little effect on the outer peak and the large scale motions.

To test the influence of the detection location on the flow structures, two higher detection planes are chosen at $y^+ = 30$ and $y = 0.1h$, which are the top of the buffer layer and in the the logarithm region, respectively. As shown in figure 5(a), the locations of outer peaks of maximum transient growth under $y_d^+ = 30$ control are unchanged. Similar to the cases of $y_d^+ = 15$ control, the difference of the outer peak values between the no control case and the controlled case decreases as the Reynolds number increases. However, the outer peak values under $y_d^+ = 30$ are suppressed more than that $y_d^+ = 15$

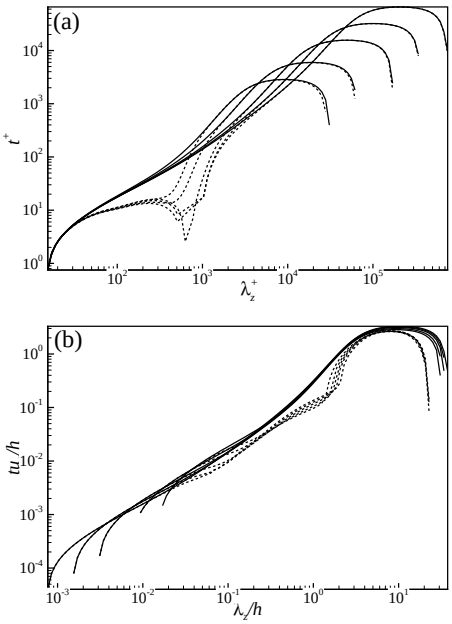

Figure 6. Variations of T_{max} as a function of λ_z for $\alpha = 0$ at $Re_\tau = 500 \sim 20000$. (a) $y_d^+ = 30$, λ_z is scaled in wall units ν/u_τ; (b) $y_d = 0.1h$, λ_z is scaled in h. Solid lines represent the no control cases and dashed lines stand for the control cases.

control for $Re_\tau < 5000$, indicating that with the elevation of the detection plane, the influence of the control on large scale motion becomes more obvious. For example, the outer peak value at $Re_\tau = 500$ under $y_d^+ = 15$ control and $y_d^+ = 30$ control are 9 and 7, respectively. Notably, the influence of $y_d^+ = 30$ control is also insignificant for even larger Reynolds number. The diminishing of the inner peak by the $y_d^+ = 30$ control is less effective than by the $y_d^+ = 15$ control. The inner peaks locating at $\lambda_z^+ \approx 92$ in the no control cases moves to $\lambda_z^+ \approx 50$ for all the Reynolds numbers in the $y_d^+ = 30$ control cases. The time to reach the maximum transient growth under $y_d^+ = 30$ control is shown in figure 6(a). Compared with the $y_d^+ = 15$ control, the influence of the $y_d^+ = 30$ control on T_{max} covers a larger spanwise wavelength range but is still limited in the small-scale structures. Therefore, the control restricted in the buffer layer, such as $y_d^+ = 15$ and $y_d^+ = 30$ control, has limited influence on the large scale structures, especially at high Reynolds numbers, but can obviously suppress the near-wall scale structures.

When the detection plane is located in the logarithm region, the influence of the control on large scale structures is much more obvious. As shown in figure 5(b), although the outer peak locations under $y_d = 0.1h$ control are the same as the case of no control, the values of the outer peaks are much smaller. Moreover, different from the control with detection plane located in the buffer layer, the suppression of the outer peak is independent of the Reynolds number. The reason lies in that the detection location is scaled in outer length scale h. The transient growth process under the control is still that the amplified streaks capture energy from the initial vortices. The distributions of the optimal initial vertical velocity and the amplified streamwise velocity are shown

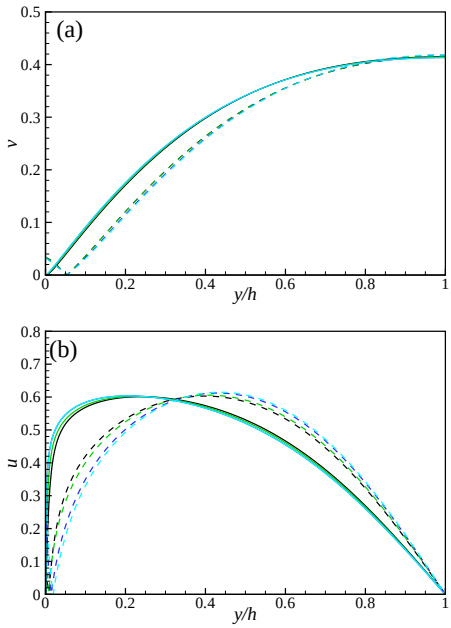

Figure 7. Distributions of (a) optimal initial vertical velocity, (b) amplified streamwise velocity for no-slip case (solid line) and $y_d = 0.1h$ control (dashed line) for $\alpha h = 0$, $\beta h = 1.5$ at $Re_\tau = 1000 \sim 5000$.

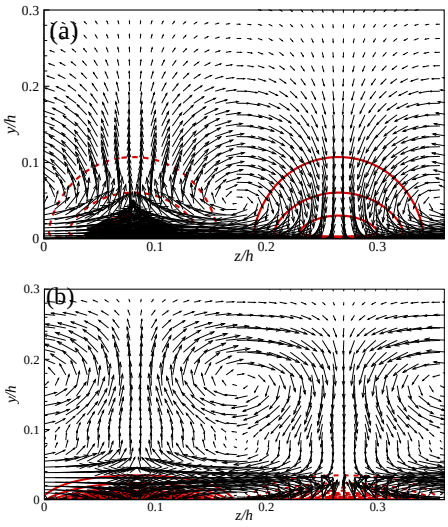

Figure 8. vectors for optimal initial velocity filed and contours for amplified streamwise velocity at controlled new peak for (a) no control case and (b) $y_d = 0.1h$ control. The dashed line indicates negative streamwise velocity and solid line represents positive streamwise velocity.

in figure 7(a) and (b), respectively, for the no control and the $y_d = 0.1h$ control cases. The optimal initial vertical velocity for different Reynolds numbers collapses into one curve under $y_d = 0.1h$ control, which means the controlled optimal initial structures are similar. Compared with the no control case, the controlled optimal initial vertical velocity is suppressed in a large range in the vertical direction. This may lead to the decrease of G_{max}, because the energy of the amplified streaks is captured from the mean flow through the initial vortices. Since the term $-i\beta\hat{v}DU/D\eta$ causes the non-normality of the linearized equations for the perturbations and leads to the transient growth, the decrease of vertical velocity below $y = 0.3h$ can make the location of maximum $-i\beta\hat{v}DU/D\eta$ move away from the wall. Therefore, the location of the amplified streaks may be shifted away from the wall. Additionally, due to the similarity of the initial vortices, the distribution of the amplified streaks for all the Reynolds numbers considered in the present work should be also similar. This has been confirmed by figure 7(b). The location of the maximum streamwise velocity is shifted from $y = 0.1h$ in the no control cases to $y = 0.4h$ under the $y_d = 0.1h$ control for all the Reynolds numbers considered, and different from the no control cases, the streaks do not penetrate into the near-wall region. As shown in figure 6(b), under $y_d = 0.1h$ control the time to reach the maximum transient growth at the spanwise wavelength of the outer peak is only a little bit smaller than the no control case. The almost identical time but obviously smaller peak value for the transient growth under $y_d = 0.1h$ control indicates that the suppression of the outer peak is effective.

Although the $y_d = 0.1h$ control can greatly suppress the original outer large scale motions, it also produces a new peak in G_{max} around $\beta h \approx 19$, where the transient growth rate is small in the no control cases, as shown in figure 5(b). The initial optimal vectors and amplified streaks for the no control case and $y_d = 0.1h$ control at $\beta h \approx 19$ are shown in figures 8(a) and (b), respectively. The control pushes up the bottom of the initial vortices to $y = 0.035h$, below which there are semi-vortices induced by the opposition control. Hence, the location of the initial vortices under $y_d = 0.1h$ control is higher than that in the no control case. Different from the no control case, there are two vortex cores in the vertical direction above $y = 0.035h$. Moreover, it is significant that the locations of the most amplified streaks are changed by the control. In the no control case, the amplified streaks are extended to $y = 0.1h$, although it deeply penetrates into the near-wall region. However, under $y_d = 0.1h$ control, the streaks are most amplified in the region below $y = 0.035h$ which is dominated by the opposition control, and the amplification of the initial vortices is suppressed. Notably, the vertical velocity around $y = 0.1h$ is large for both the no control and the control cases, and hence the vertical velocity on the wall is also of large amplitude. Consequently, the term $-i\beta\hat{v}DU/D\eta$ is also significant near the wall, resulting in the great transient growth of the perturbations there. We also tested the control with the even higher detection locations above the center of the logarithm region, such as $y_d = 0.2h$, and found it resulted in the computational instability. Therefore, to suppress the large scale motion the detection location should be scaled in h and should be in the lower part of the logarithm region.

Because the amplitudes of the blowing/suction velocity at the wall in $y_d = 0.1h$ control are larger than that in the $y_d^+ = 15$ and 30 controls, and the $y_d = 0.1h$ control are much more effective in suppressing the large scale motion than the $y_d^+ = 15$ and 30 controls. It should be clarified whether the amplitude or the phase of the control is crucial for the suppression of the large scale motion. Hence, the $y_d^+ = 15$

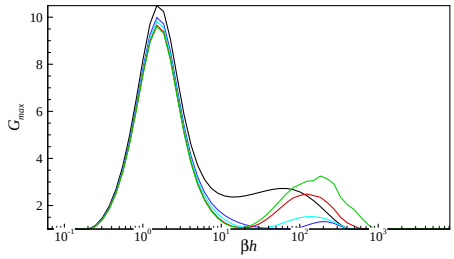

Figure 9. Distribution of G_{max} as a function of β at $\alpha = 0$ and $Re_\tau = 1000$ for the cases of no control and strengthened $y_d^+ = 15$ controls with $A = 1, 2, 5, 8$.

controls with strengthened control amplitude are checked at $Re_\tau = 1000$. In this case, the wall blowing/suction velocity is determined by $\hat{v}_{wall} = -A\hat{v}(y_d)$, in which A is the amplitude parameter. The transient growth rates in the cases of the strengthened control with $A = 1, 2, 5, 8$ are shown in figure 9. The location as well as the value of the outer peak changes very little by the strengthened control in comparison with the no control case. For other Reynolds numbers, the results are also similar. This suggests that the control with input signal detected in the buffer layer, even with an increased amplitude, can hardly affect the large scale motion, indicating that the detection location is a crucial factor to achieve effective manipulation of the large scale motions.

Summary

The linear transient growth model is employed to study the effect of active control on flow structures in wall turbulence. The control with $y_d^+ = 15$ can significantly suppress the transient growth of the near-wall structures, but the control with the detection plane located in the buffer layer has very limited influence on the large scale motions, even the control amplitude is increased. Taking the information at $y + 0.1h$ in the logarithm region as the input signal, the control is very effective in suppressing the large scale motions corresponding to the outer peak in the maximum transient growth rate. With this high detection location, new peak occurs in the transient growth rate, caused by the strong manipulation on the wall. The energy amplification of the optimal initial structures further away from the wall is still suppressed. These results suggest that the effect of the control on the large scale motion mainly depends on the detection location.

Acknowledgement

The work is supported by National Science Foundation of China (Grant No. 10925210, 11132005).

REFERENCES

Abe, H., Kawamura, H. & Choi, H. 2004 Very large-scale structures and their effects on the wall shear-stress fluctuations in a turbulent channel flow up to re_τ =640. *Trans. ASME: J. Fluid Engng* **126**, 835–843.

Adrian, R. J., Meinhart, C. D. & Tomkins, C. D. 2000 Vortex organization in the outer region of the turbulent boundary layer. *J. Fluid Mech.* **422**, 1–54.

del Alamo, J. C. & Jimenez, J. 2003 Spectra of the very large anisotropic scales in turbulent channels. *Phys. Fluids* **15**, L41–L44.

del Alamo, J. C. & Jimenez, J. 2006 Linear energy amplification in turbulent channels. *J.Fluid Mech.* **559**, 205–213.

Butler, K. M. & Farrell, B. F. 1992 Three-dimensional optimal perturbations in viscous shear flow. *Phys. Fluids* **4**, 1637–1650.

Butler, K. M. & Farrell, B. F. 1993 Optimal perturbations and streak spacing in wall-bounded turbulent shear flow. *Phys. Fluids A* **5**, 774–777.

Choi, H., Moin, P. & Kim, J. 1994 Active turbulence control for drag reduction in wallbounded flows. *J. Fluid Mech.* **262**, 75–110.

Collis, S. S., Seifert, A. R. D. & Theofilis, V. 2004 Issues in active flow control: theory, control, simulation, and experiment. *Prog. Aero. Sci.* **40**, 237–289.

Gnanpathisubramani, B., Hambleton, N., Hutchins, W. T., Longmire, E. K. & Marusic, I. 2005 Investigation of large-scale coherence in a turbulent boundary layer using two-point correlation. *J. Fluid Mech.* **524**, 57–80.

Hoyas, S. & Jimenez, J. 2006 Scaling of the velocity fluctuations in turbulent channels up to $re_\tau = 2003$. *Phys. Fluids* **18**, 011702.

Kravchenko, A. G., Choi, H. & Moin, P. 1993 On the relation of near-wall streamwise vortices to wall skin friction in turbulent boundary layers. *Phys. Fluids A* **5**, 3307–3309.

Lim, J. & Kim, J. 2004 A singular value analysis of boundary layer control. *Phys. Fluids* **16**, 1980–1988.

O.Flores, J. Jimenez & del Alamo, J. C. 2007 Vorticity organization in the outer layer of turbulent channels with disturbed walls. *J.Fluid Mech.* **591**, 145–154.

Pujals, G., Garcia-Villalba, M., Cossu, C. & Depardon, S. 2009 A note on optimal transient growth in turbulent channel flows. *Phys. Fluids* **21**, 015109.

Robinson, S. K. 1991 Coherent motions in the turbulent boundary layer. *Annu. Rev. Fluid Mech.* **23**, 601–639.

Schmid, P. J. & Henningson, D. S. 2001 Stability and transition in shear flows. In *Stability and Transition in Shear Flows*. Springer.

Tomkins, C. D. & Adrian, R. J. 2003 Spanwise structure and scale growth in turbulent boundary layers. *J. Fluid Mech.* **490**, 37–74.